AWARD NUMBER: W81XWH-20-1-0899

TITLE: Portable Diffuse Optical Sensors for Point-of-Care Monitoring in Prolonged Field Care

PRINCIPAL INVESTIGATOR: Dr. Kurtulus Izzetoglu

CONTRACTING ORGANIZATION: Drexel University, Philadelphia, PA

REPORT DATE: October 2021

TYPE OF REPORT: Annual Report

PREPARED FOR: U.S. Army Medical Research and Development Command
Fort Detrick, Maryland 21702-5012

REPORT DOCUMENTATION PAGE

Form Approved
OMB No. 0704-0188

1. REPORT DATE	**2. REPORT TYPE**	**3. DATES COVERED**
October 2021	Annual	30Sep2020-29Sep2021

4. TITLE AND SUBTITLE

Portable Diffuse Optical Sensors for Point-of-Care Monitoring in Prolonged Field Care

5a. CONTRACT NUMBER
W81XWH-20-1-0899

5b. GRANT NUMBER

5c. PROGRAM ELEMENT NUMBER

6. AUTHOR(S)
Dr. Kurtulus Izzetoglu

E-Mail: ki25@drexel.edu

5d. PROJECT NUMBER

5e. TASK NUMBER

5f. WORK UNIT NUMBER

7. PERFORMING ORGANIZATION NAME(S) AND ADDRESS(ES)

Drexel University
3141 Chestnut St
Philadelphia, PA 19104-2816

8. PERFORMING ORGANIZATION REPORT NUMBER

9. SPONSORING / MONITORING AGENCY NAME(S) AND ADDRESS(ES)

U.S. Army Medical Research and Development Command
Fort Detrick, Maryland 21702-5012

10. SPONSOR/MONITOR'S ACRONYM(S)

11. SPONSOR/MONITOR'S REPORT NUMBER(S)

12. DISTRIBUTION / AVAILABILITY STATEMENT

Approved for Public Release; Distribution Unlimited

13. SUPPLEMENTARY NOTES

14. ABSTRACT

The main purpose is to develop the prototype of a portable diffuse correlation spectroscopy (DCS) and near infrared spectroscopy (NIRS) based optical system with multiple capabilities to monitor: cerebral and somatic oximetry; cerebral and somatic blood flow and volume; and cerebral edema. The proposed system will include multi-distance multi-wavelength NIRS-based sensors and DCS-based optical fibers. The proof of concept and system test studies include design and study of phantom and animal models, tests in hemorrhage assessment during pre-shock, shock, after fluid resuscitation; and during hypoxia and edema development. Final proof of concept study will be conducted using a real-life clinical scenario with adult pig model (uncontrolled hemorrhagic shock). A fully operational DCS optical system with all the components including the sensor array, data acquisition box and software was developed in Year 1. The novel head phantoms and dynamic microvasculature model (mimicking adult human head with extracerebral layers) were also designed and implemented to model varying cerebral blood volume and cerebral blood flows. Animal models and test plans are also developed for graded hemorrhage. The data collection with intralipids and blood is completed, and the results validate that the prototype system is capable of measuring microvascular blood flow rate, volume and oxygenation changes.

15. SUBJECT TERMS

Prolonged field care, point-of-care imaging, diffuse correlation spectroscopy, DCS, near infrared spectroscopy, NIRS, traumatic brain injury, hemorrhagic shock.

16. SECURITY CLASSIFICATION OF:			**17. LIMITATION OF ABSTRACT**	**18. NUMBER OF PAGES**	**19a. NAME OF RESPONSIBLE PERSON**
a. REPORT	**b. ABSTRACT**	**c. THIS PAGE**			USAMRMC
Unclassified	Unclassified	Unclassified	Unclassified	**39**	**19b. TELEPHONE NUMBER** *(include area code)*

TABLE OF CONTENTS

1. **INTRODUCTION:**

The ability to combine local microcirculatory blood flow measures (which is the critical physiological biomarker for various injuries, in particular, hemorrhagic shock) and local tissue oxygen saturation via hemoglobin oxygenation and deoxygenation lends itself to an advanced approach and accelerated medical device development, specifically for a point-of-care monitoring in prolonged field care. The main purpose is to develop the prototype of a portable diffuse correlation spectroscopy (DCS) and near infrared spectroscopy (NIRS) based optical system with multiple capabilities to monitor: cerebral and somatic oximetry; cerebral and somatic blood flow and volume; and cerebral edema. The proof of concept and system test studies include design and study of dynamic phantom models mimicking brain tissue and animal models for the tests in hemorrhage assessment during pre-shock, shock, after fluid resuscitation as well as during hypoxia and edema development. Final proof of concept study will be conducted using a real-life clinical scenario with adult pig model for the uncontrolled hemorrhagic shock.

2. **KEYWORDS:**

Prolonged field care, diffuse correlation spectroscopy, DCS, near infrared spectroscopy, NIRS, TBI, hemorrhagic shock, local tissue oxygenation, blood flow index.

3. **ACCOMPLISHMENTS:**

What were the major goals of the project?

Major Goals & SOW Tasks	**Timeline (Month)**	**Progress**
Aim 1 - Develop and test the prototype of the integrated diffuse correlation spectroscopy (DCS) - near infrared spectroscopy (NIRS) DCS-NIRS system		
Major Task 1. Develop & Test Prototype	1-12 Month	In Progress
Subtask 1.1: Develop the sensors and control box unit of the DCS system.	1-3 Month	100% (Complete)
Subtask 1.2: Re-design and develop an oximetry/edema board (NIRS system) by implementing new digital lock-in amplifiers.	2-6 Month	100% (Complete)

Subtask 1.3: Integrate DCS hardware components into NIRS system.	3-12 Month	75% (In Progress)
Subtask 1.4: Perform initial prototype testing with phantoms, including but not limited to: *a. initial system tests on linearity, drift, depth of penetration, and noise analysis* *b. device performance evaluation in terms of repeatability and accuracy under hypoxia, ischemia, varying blood flow and edema development conditions.*	6-12 Month	75% (In Progress) *a. 100% (Complete)* *b. 50% (*In Progress*)*
Aim 2 - Perform animal tests for feasibility and validation		
Major Task 2. Test prototype in piglet model	1-15 Month	In Progress
Subtask 2.1 Prepare and submit the research protocol with animals for the review and approvals by IACUC and ACURO.	1-6 Month	**100% (Complete)**
Subtask 2.2 Test prototype in piglet model of graded hemorrhage: *a. Measure physiological data, including but not limited to heart rate (HR), blood pressure (BP), pulse oximetry; and DCS-NIRS somatic and cerebral signals for the tissue oximetry, blood flow and blood volume.* b. *Analyze physiological data and DCS-NIRS signal synchrony in response to change in the phase of hemorrhagic shock.*	9-15 Month	0% (Not Yet Initiated) a. *0% (Not Yet Initiated)* b. *0% (Not Yet Initiated*
Subtask 2.3 Test the prototype for changes in cerebral and somatic signals following cerebral edema development in a piglet model of	9-15 Month	0% (Not Yet Initiated)

hypoxia-induced cerebral edema: *a. Measure intracranial pressure (ICP), and physiological data including but not limited to HR, BP, pulse oximetry, and DCS-NIRS signals for the tissue oximetry, blood flow, blood volume and water content.* *b. Analyze to determine the relationship between changes in DCS-NIRS signals of cerebral and somatic tissue oxygen saturation, cerebral edema, cerebral blood flow and changes in intracranial pressure (ICP) and pulse oximetry.* c. *Analyze physiological data and DCS-NIRS signal synchrony in response to edema development*. Subtask 2.4: Modify the prototype based on the piglet model tests.	 12-15 Month	 *a. 0% (Not Yet Initiated)* b. *0% (Not Yet Initiated)* c. *0% (Not Yet Initiated)* 0% (Not Yet Initiated)
Aim 3 - Perform validation tests with adult pig models mimicking real-life clinical scenario		
Major Task 3. Test prototype in adult pig model of controlled and uncontrolled hemorrhagic shock	12-24 Month	Not Yet Initiated
Subtask 3.1: Test the prototype in an adult pig model of controlled hemorrhagic shock. Subtask 3.2: Test the prototype in an adult pig model of uncontrolled hemorrhage by liver laceration. Subtask 3.3: System fine-tuning and final validation analysis.	12-16 Month 17-20 Month 21-24 Month	0% (Not Yet Initiated) 0% (Not Yet Initiated) 0% (Not Yet Initiated)
Aim 4 - Provide technical progress reports for the findings and system prototypes and disseminate research findings.		
Major Task 4. Reporting	3-24 Month	In Progress

Subtask 4.1 Technical progress reports (Quarterly).	3-24 Month	50% (In Progress)
Subtask 4.2 Annual technical report.	12 Month	100% (Complete)
Subtask 4.3 Prepare and disseminate findings by attending a DoD-sponsored meeting.	16-24 Month	0% (Not Yet Initiated)
Subtask 4.4 Final technical report	24 Month	0% (Not Yet Initiated)

What was accomplished under these goals?

Major Task 1. Develop & Test Prototype:

This major task was the primary focus during Year 1 with the following accomplishments and major finding: A fully operational DCS optical system with all the components including the sensor array, data acquisition box and software was developed in Year 1. The novel head phantoms and dynamic microvasculature model (mimicking adult human head with extracerebral layers) were also designed and implemented to model varying cerebral blood volume and cerebral blood flows. The data collection with intralipids and blood is completed, and the results validate that the prototype system is capable of measuring microvascular blood flow rate, volume and oxygenation changes.

Subtask 1.1: Develop the sensors and control box unit of the DCS system

The team completed this task and finalized the development of a DCS system. Figure 1 depicts the full system developed successfully with all the hardware. This system (Figure 1) enables measurement of microcirculatory blood flow tissue including human and animal head at multiple depth of penetration, up to 1-3 centimeters. The microcirculatory blood flow is quantified by illuminating tissue with a long-coherence length (>10m) near Infrared laser (785nm wavelength) with power of 120mW, which is coupled to a multimode (62.5/125μm) optical source fiber to transport light to the tissue (see Figure 1 showing power of laser source, when 785nm optical wavelength is turned on). Figure 2 reveals all the components including four-channel correlator (black box at the back).

Figure 1. The first prototype of the DCS system. The customized enclosure is designed with the dimensions of: Width x Depth x Height = 10.3”x 11.8” x 5.3".

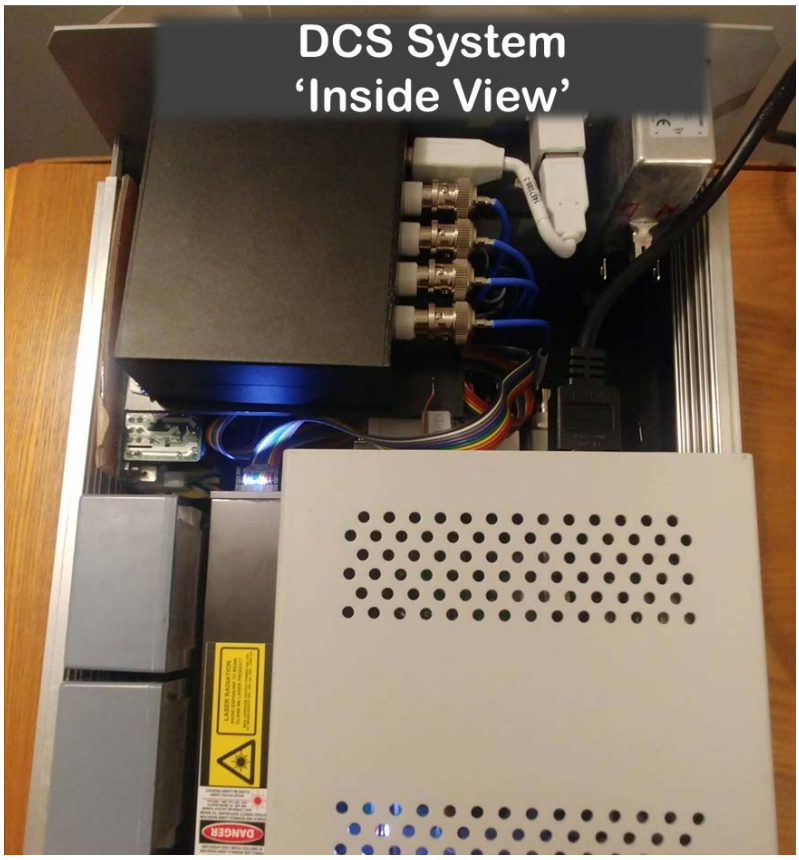

Figure 2. The system includes i. correlator for blood flow index (black box at the back); ii. Laser - 785nm wavelength with regulated emission power laser with maximum 120mW (acquired from CrystaLaser, DL785-120-SO), iii. four-channel single photon counting module (acquired from Pacer, SPCM-AQR).

Discussion: The goal was met, and a fully operational DCS optical system with all the components including the sensor array, data acquisition box and software was developed (Figures 1&2).

Subtask 1.2: Re-design and develop an oximetry/edema board (NIRS system) by implementing new digital lock-in amplifiers

To ensure reliable measures in the field, new proposed NIRS system utilizes a digital lock-in amplifier which allows the ambient light to be rejected from the actual signal and removes the requirement of measuring dark current. Hence, the team incorporated this new feature/technique (Figure 3) by using the field-programmable gate arrays (FPGA) containing an array of programmable logic blocks.

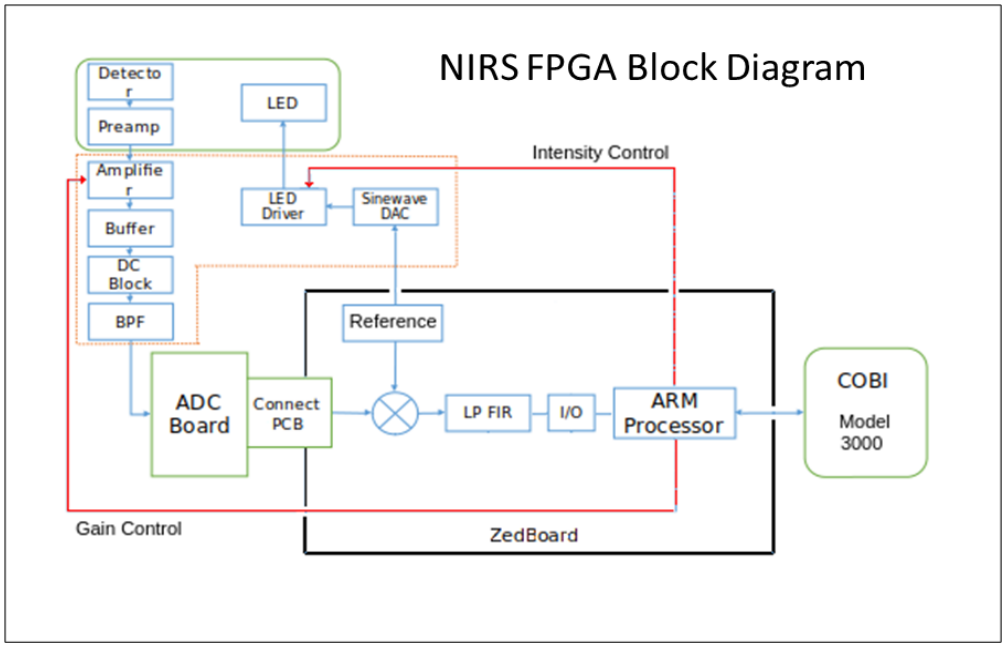

Figure 3. ***Lock-in amplifier with FPGA design***: The logic in the FPGA performs the Sine wave generation (1 KHz) and controls the analog-to-digital conversion (ADC). It multiplies the ADC outputs with the reference Sine signal and the reference Cosine signal. It also filters the resulting product data which is sent to the Arm Processor as shown in the block diagram. The ARM Processor reads the voltage of the detectors. It communicates using the current NIRS data acquisition protocol (namely, COBI protocol already developed for current and previous NIRS systems) to send detector voltages and receive commands from the user to control LED intensity and detector circuitry gain.

Discussion: Main goal was met, and design of the circuitry was completed, and the board was developed. However, the manufacturing of the printed circuit board (PCB) has been delayed and this challenge is discussed in the next subtask (Subtask 1.3)

Subtask 1.3: Integrate DCS hardware components into NIRS system
This task is to integrate hardware and software components.
Hardware integration: We have the circuitry working (Subtask 1.2) and now need manufacturing and mechanical configuration of the printed circuit boards developed in previous subtask (Figure below). The team is working on the mechanical design to fit the 4 new printed circuit boards into

the existing box (NIRS system box). The schematic, PCB fabrication, PCB assembly (Figure 4), test has been completed but manufacturing with suggested modifications has been delayed.

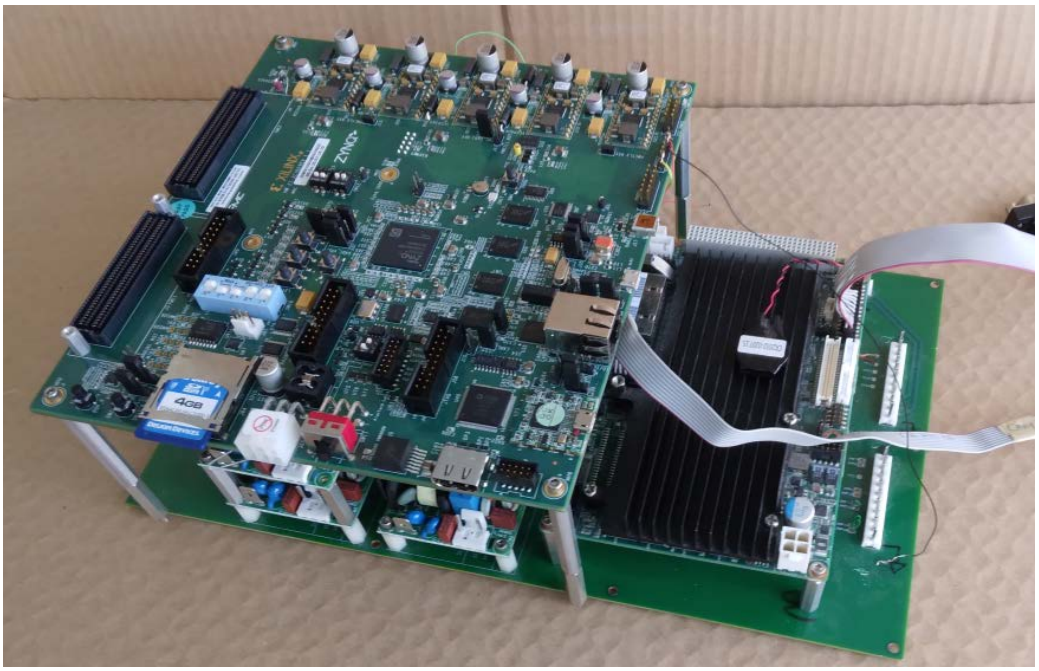

Figure 4. The prototype circuit boards assembled last quarter (Quarter 4) and suggested mechanical design to fit into current system box.

Software integration: The team has been developing a multi-threaded parallel processing architecture using current data acquisition protocol. The acquisition software, namely COBI that we developed and have been using for hematoma and local tissue oximetry detection, is utilized here for the system integration. We specifically finalized and tested a communication protocol with the data acquisition software and the new circuitry developed in this project.

Discussion: We received the first boards and mechanical designs (Figure 4) late, and found some further errors in the boards and returned with suggestions. Hence, we are still experiencing delay in the final board fabrication and mechanical configuration.

Subtask 1.4: Perform initial prototype testing with phantoms

We have evaluated the operational system performance of the proposed system under various conditions by using laboratory head models (phantoms). Prior to the animal testing, such system performance evaluations in terms of its operational characteristics including *linearity* and *resolution* are critical to characterize to develop analysis methods and optimize use of the system. In this annual report, we first summarize these initial phantom tests on photon counts and correlator function recordings as measured by the DCS device at different laser power, source detector separations, tissue scattering coefficients and flow rates. During the Quarter 4, as a next step we have also developed the algorithms and data processing codes to estimate the ***blood flow index*** (BFI) which is known to correlate with ***cerebral blood flow*** (CBF) from multi-distance DCS measurements. To determine BFI, we have performed non-linear fitting operation between the theoretical and measured signals by implementing optimization techniques to minimize the

difference between the analytical diffusion equation solution and the measured autocorrelation function, respectively (Appendix A). We performed and completed phantom tests to evaluate the performance of the BFI extraction algorithms and further collected data with the DCS and the current NIRS system simultaneously. Their combined performance is also reported in this annual report.

Discussion: The phantom tests are completed, and results are discussed below in detail with the data. We could not conduct system performance tests including newly developed boards as we experience production delay. This challenge is reported, and the details are provided in Subtask 1.3.

a. *(Subtask 1.4.a) Initial system tests on linearity, drift, depth of penetration, and noise analysis*

Linearity test: We first evaluated whether the DCS system satisfied the desired linear relationship between the input light power and the photon counting outputs of the avalanche photodiode (*APD*) is at various source-detector separations (SDS) within the operational light input ranges of the device. These tests guarantee that any changes measured by the device is not confounded by a non-linear relationship between the input light power and the photon count outputs of the device.

The phantom and overall experimental setup are provided in Figures 5(a) and (b). For these tests, we prepared a liquid phantom by mixing 30 mL of Intralipid (20% fat emulsion) in 1000 mL water in a large beaker to obtain a reduced scattering coefficient of μ_s'=6cm-1 in the phantom with this 3% Intralipid mixture. Once the liquid phantom was prepared, the beaker was placed on a magnetic stirrer which was turned on in between measurements to keep the mixture homogeneous by stirring it constantly and turned off during measurements not to cause unintended movement in the liquid which could be detected by the DCS system. Temperature during the measurements were at the room temperature level of ~25 ^{o}C.

Using a holder, the sensor is positioned on top of the liquid phantom at a depth allowing the light source and the detectors make good contact with the liquid but not fully dipping the overall sensor in the phantom. The recordings are collected for the SDS at 25, 30 and 37mm, and for the driving power of the laser and hence the intensity of incident light increased from 10 mW to 100mW at 5 mW intervals. We also turned the ambient light off during data collection to reduce any light leakage to the detectors. Figure 6 presents the input laser power vs the measured photon counts as detected by the APD at various SDS together with the best line fit. *These results verified linear operation characteristics of the DCS system between output photon counts and the input laser power.*

Figure 5. (Left) Liquid phantom and DCS sensor; (Right) Experimental test setup

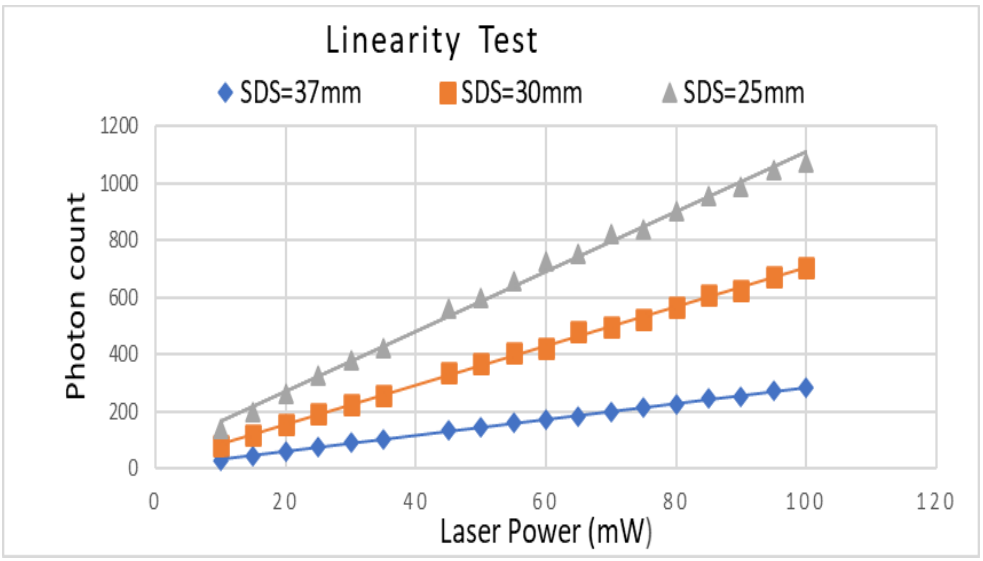

Figure 6. Photon counts versus laser power as measured by the DCS system at different depth of penetration determined by different source-detector separations (SDSs).

Scattering titration test: Next, we implemented the intralipid titration test similar to the study by Tamborini et al. 2017. In this test, we used the same experimental setup as in linearity test and prepared liquid phantoms with 1%, 2% and 3% Intralipid concentrations in 1000mL water modeling μ_s' of 2 cm^{-1}, 4 cm^{-1}, and 6 cm^{-1}, respectively. Figure 7 presents the semi-log plot of the measured temporal autocorrelation function, $g_2(\tau)$ at varying logarithmic delay times for different reduced scattering coefficients at 25 mm SDS. As expected, $g_2(\tau)$ showed an initial constant plateau but decayed exponentially with increasing delay time. It is known that when the medium gets more scattering, the temporal autocorrelation function decays earlier (Vishwanath, et al., 2019). *Our findings in this scattering titration test using our DCS system were in agreement with these theoretical expectations, hence validating its acceptable operation.*

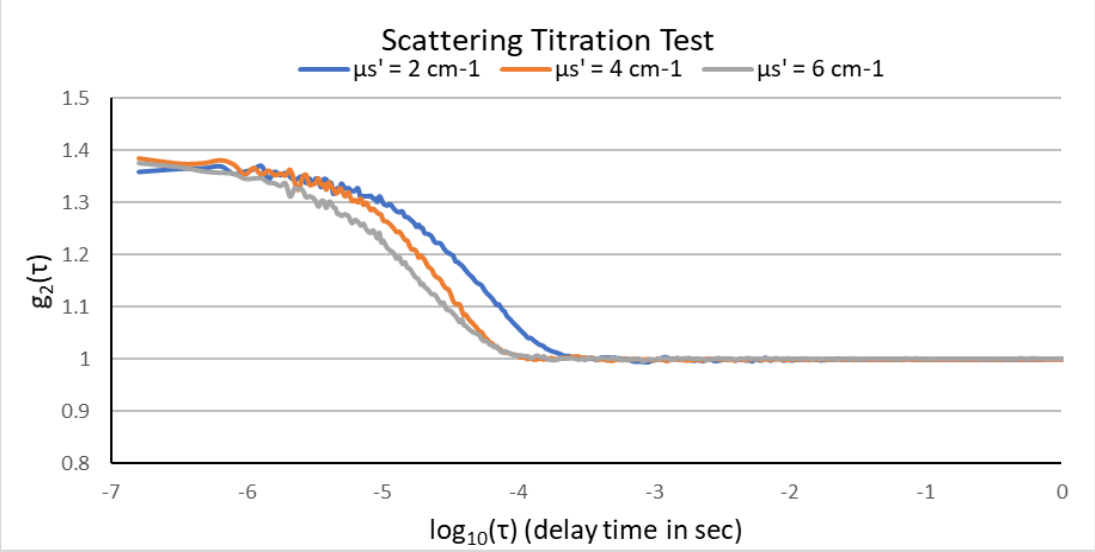

Figure 7. The logarithmic delay time versus the measured temporal autocorrelation function, $g_2(\tau)$ for different reduced scattering coefficients obtained using the scattering titration test.

Flow speed tests: In this test we evaluated the performance of the prototype DCS system in tracking changes of the flow rate using a liquid microvasculature phantom model. The team designed and custom developed a tissue-like phantom mimicking the anatomical structure of microvasculature using fluid channels. These fluid channels (capillaries) are made using flexible tubing while controlling the flow of liquid material at different rates in order to model the movement of RBC.

We built the dynamic microvasculature phantom as a one-layer head phantom initially to verify that the device is capable of reflecting microvascular blood flow rate changes in its measurements without the head layer effects to be considered. However, note that multilayer versions of the proposed dynamic phantom can also be built and evaluated in the future. The newly designed and developed phantom and the overall experimental setup are depicted in Figure 8. The phantom is consisted of:

i. an embedded structure to mimic the microvasculature with fluid channels which is made from clear and flexible platinum/silicone tubing (inner diameter = 1.6 mm, outer diameter = 3.2 mm, Nordson medical, SILC7001657) bent several times and attached to a circular iron wire support with legs (Figure 8(a)).
ii. a cube shaped plexiglass container (an aquarium) to build the liquid phantom mimicking the head with the embedded microvasculature structure placed inside it.
iii. NE-300 Infusion™ Syringe Pump with adjustable infusion rates from 0.73 µL/hr (1 mL syringe) to 1500 mL/h (60 mL syringe) to model blood flow within the microvasculature at different flow rates.

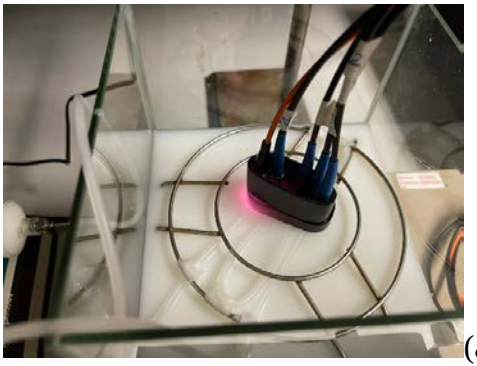
(a)

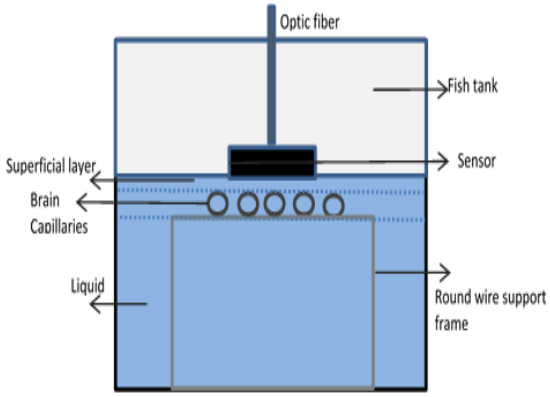

(b)

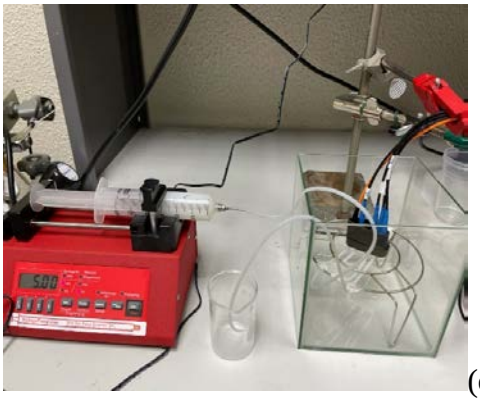
(c)

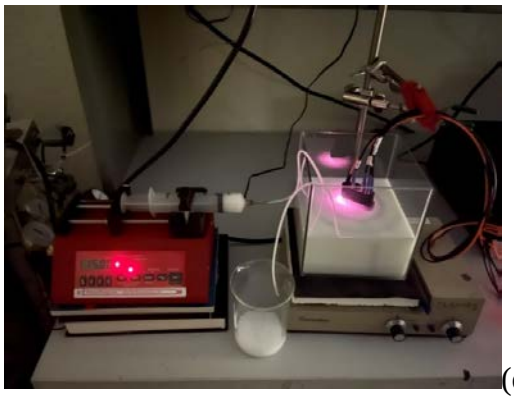
(d)

Figure 8. (a) Dynamic microvasculature phantom model; (b) Embedded microvasculature structure with tubing attached to wire support; (c) Experimental setup without liquid phantom mixture; (d) Overall view of setup during experimentation.

With this setup (Figure 8), the temporal autocorrelation function, $g_2(\tau)$ was recorded at various SDS separately for *distinct flow rates* including the baseline (0 mL/h), 50 mL/h, 100 mL/h and 150 mL/h, Figure 9 presents the logarithmic delay time ($\log_{10}(\tau)$) versus the measured temporal autocorrelation function, $g_2(\tau)$ for different flow rates at 25 mm SDS. In Figure 10, we also presented temporal autocorrelation ($g_2(\tau)$) measurements at two SDS (25 mm vs 30 mm) at different flow rates separately to investigate the effect of SDS on DCS measurements. *Our DCS system temporal autocorrelation measurements were able to reflect the expected alterations when the flow rate or the SDS were changed. As speed (flow rate) increased, we observed sharp decay (Figure 9, see fast flow vs slow flow). When the SDS, i.e., depth of penetration, is increased the measures started to decay earlier as compared to lower values, which are corresponding to the measures from the region closed to extracerebral layers (Figure 10; see different depth of penetration by varying SDSs with fixed flow rates).*

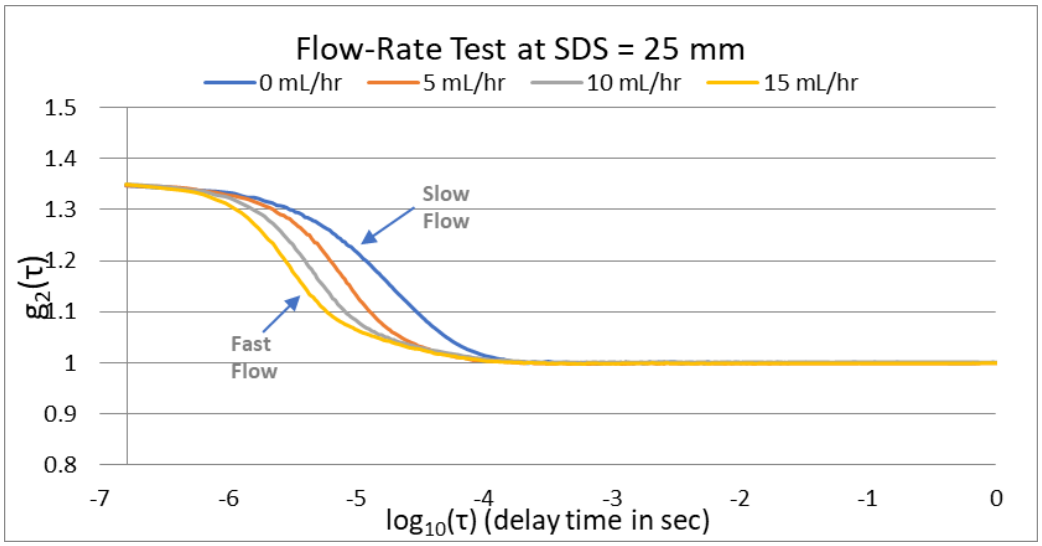

Figure 9. The logarithmic delay time versus the measured temporal autocorrelation function, $g_2(\tau)$ for different flow rates at 0, 50, 100 and 150 mL/h.

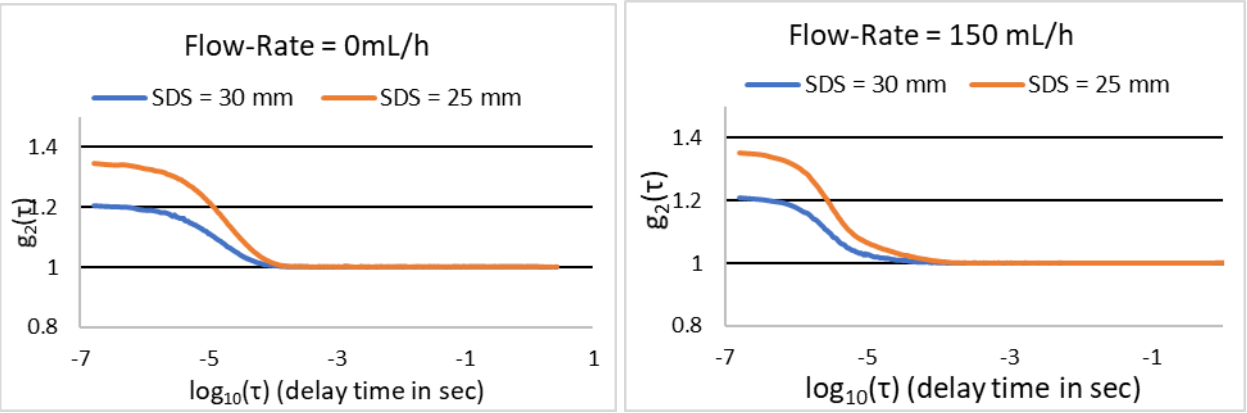

Figure 10. The logarithmic delay time ($\log_{10}(\tau)$) vs. the measured temporal autocorrelation function, $g_2(\tau)$ for two different flow rates at 0, 150 mL/h, and two different source detector separations; 25 and 30 mm.

b. *(Subtask 1.4.b) Device performance evaluation in terms of repeatability and accuracy under hypoxia, ischemia, varying blood flow and edema development conditions.*

Blood flow index carry information on alterations in cerebral blood flow (CBF) due to physiological or disease related conditions. We implemented the theory that DCS measures the speckle fluctuations over time due to the moving scatterers in tissue (such as red blood cells -RBC), which is then used to estimate an index of blood flow in the microvasculature, namely the blood flow index (BF_i). We developed algorithm and the analysis codes to determine blood flow index (BF_i). The additional test data, theoretical information, the equations we used, and citations are provided in ***Appendix A***.

Simultaneous Blood Flow (DCS system) and Oxygen Saturation (NIRS System) Measures: The overall experimental setup we used to evaluate DCS system measurements together with an NIRS system is shown in Figure 11. Note that this NIRS system does not include newly developed boards as we experience delay in manufacturing of these boards. By using liquid phantom we modelled the changes in tissue absorption (μ_a) and tissue scattering, (μ_s') and regional oxygen saturation (rSO2). We first placed the sensor of the NIRS system on the round measurement window located on one side of the liquid phantom as shown on the right in Figure 11 (Right: NIRS sensors covered by black band to fix onto the side of window). Then, we placed the DCS sensor where the light source and detectors touching the liquid phantom solution surface. The NIRS device used in these tests is composed of two identical sensors housing one light source with three built in light emitting diodes (LEDs) at 730, 850 and 940 nm (for edema measures) wavelengths.730nm and 850nm are for regional oxygen saturation (rSO2) measures, 940nm is for edema monitoring.

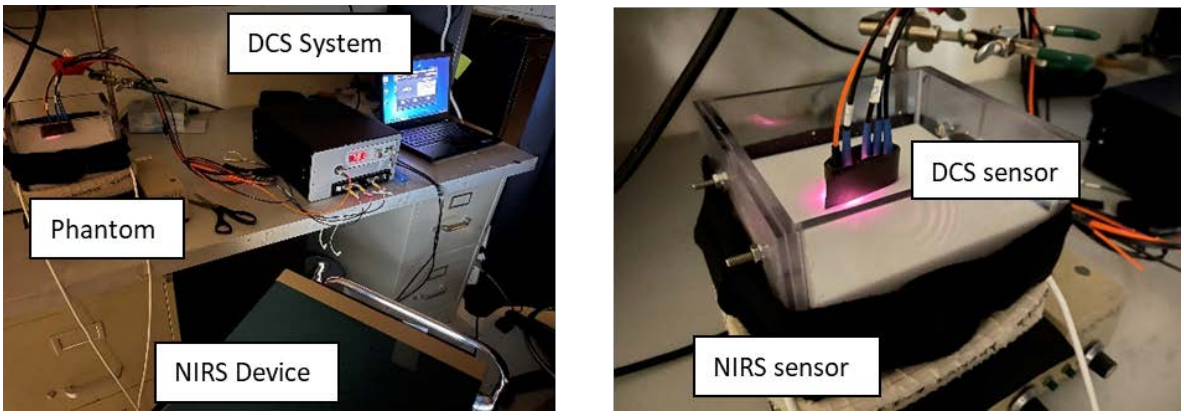

Figure 11. (Left) Test setup for simultaneous DCS and NIRS recordings. (Right) Liquid phantom with DCS and NIRS sensors where changes in tissue absorption (μ_a) and tissue scattering, (μ_s') and oxygen saturation (rSO2) are modeled.

Intralipid titration test and phantom preparation: Dynamic liquid phantoms are prepared with appropriate amounts of the absorbing agent, India ink (Black India 44201, Higgins, MA, USA) and the scattering agent, Intralipid (A 20% I.V. fat emulsion in Excel container, Fresenius Kabi) in 2000ml of water to prepare the starting absorption and scattering coefficients of $\mu_a = 0.1$ cm^{-1} and $\mu_s' = 4$ cm^{-1}, respectively. The phantom was placed on a magnetic stirrer used to keep the liquid inside the phantom homogeneous and the temperature was at 23^{o}C. While keeping the μ_a constant, we added certain percentages of Intralipid to the liquid phantom solution every 4 min to increase μ_s'

inside the phantom in steps of 2 cm^{-1} for a total of 8 stages. Hence, with this phantom, we tested the simultaneously recorded DCS and NIRS measurements for the consecutively increased reduced scattering parameters of μ_s'=4, 6, 8, 10, 12, 14, 16 and 18 cm^{-1}.

NIR Device Measurements - Intensity and ΔOD: In Figure 12, we present the intensity measurements as recorded by the NIRS device at 730, 850 and 940nm wavelengths from its detectors at (a) 25 mm and (b) 36 mm SDS. *It can be clearly seen that when the scattering, μ_s' in the medium is increased the measured intensity levels decreased as light gets diffused more.*

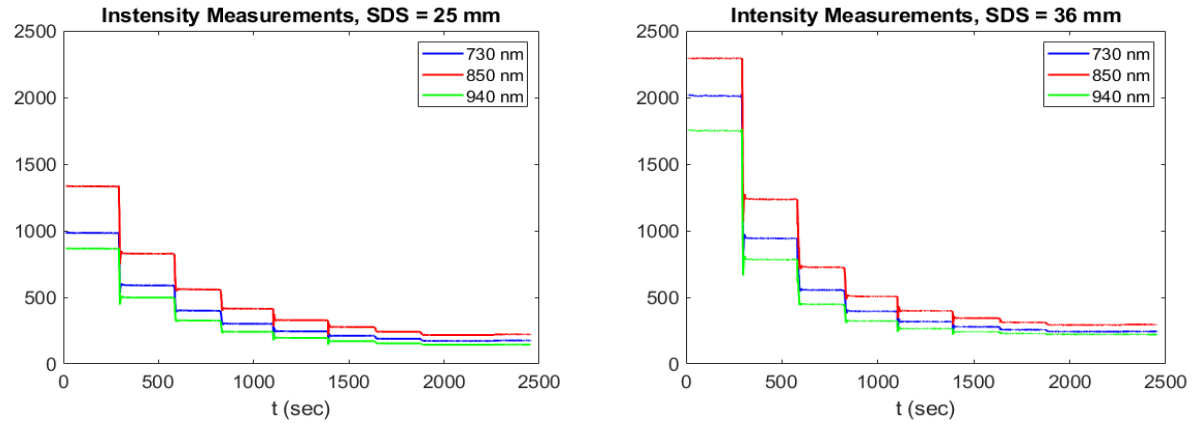

Figure 12. Raw intensity measurements for light sources at 730, 850 and 940 nm wavelengths measured from detectors at 25 and 36 mm SDS during Intralipid titration test.

We also extracted the change in optical density (Δ*OD*) which is defined as $\Delta OD = -log_{10}(I_t/I_b)$ where I_t is the intensity measurements during the test and I_b is the intensity measurement during a baseline condition. Taking two seconds of data in the beginning of the recordings when $\mu_s' = 4$ cm^{-1} as baseline region, the calculated Δ*OD* values at each wavelength and SDS are shown in Figure 13. *As expected, the attenuation in the medium is increased as the scattering, μ_s' increased.*

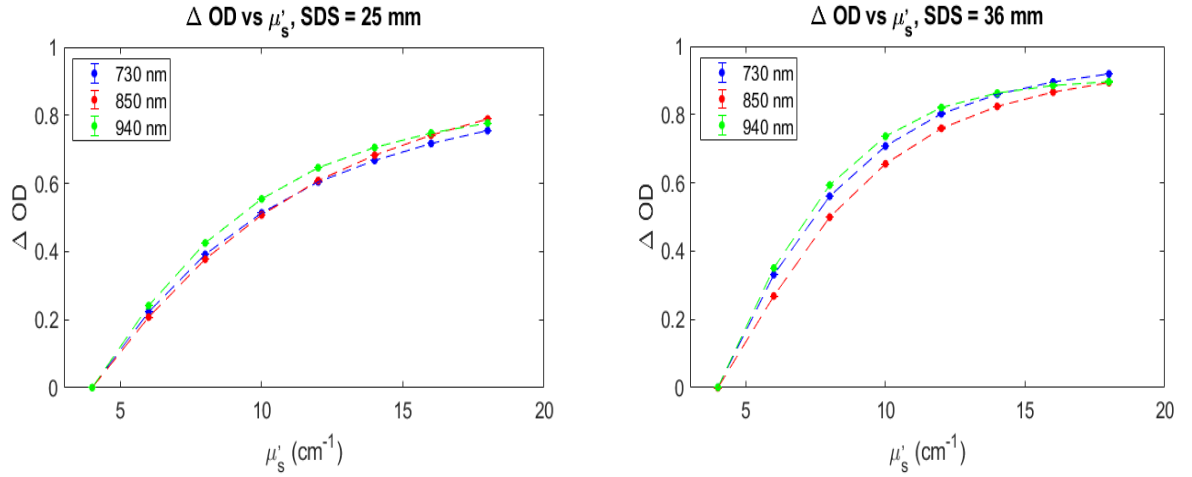

Figure 13. Changes in optical density measurements, Δ*OD* versus scattering, μ_s' for light sources at 730, 850 and 940 nm wavelengths measured from detectors at 25 and 36 mm SDS.

Oxygenation test, blood phantom preparation and experimental setup (hypoxia model through oxygenation and deoxygenation): First, the base liquid phantom is prepared using appropriate amount of Intralipid (A 20% I.V. fat emulsion in Excel container, Fresenius Kabi) in 2000ml of water to reach scattering coefficients of $\mu_s' = 8$ cm^{-1} at 780 nm wavelength. Next, two packets of phosphate-buffered saline powder (Sigma-Aldrich P3813-10PAK) were added to achieve the pH level of ~7.4. Then, DCS and NIRS sensors are placed on the two outside walls of the phantom (Figure 14).

Once the sensors are in place, we added fresh whole bovine blood of 50 mL to the mixture to achieve total hemoglobin concentration (ctHb) of ~57 μM in the liquid phantom similar to humans (Figure 15). Since the mixture is exposed to room air on top of the container, the blood in the phantom should equilibrate in few minutes and reach to > 90% hemoglobin oxygen saturation. We then cover the phantom container using a custom-made lid and added 8 g yeast to be able to induce deoxygenation in the liquid phantom for ~20 min. Once the steady state level of deoxygenation of approximately <10% levels is reached we turn on the oxygen tank, to speed up the oxygenation process until a state level of re-oxygenation is reached. The temperature of the liquid was kept at ~23ºC.

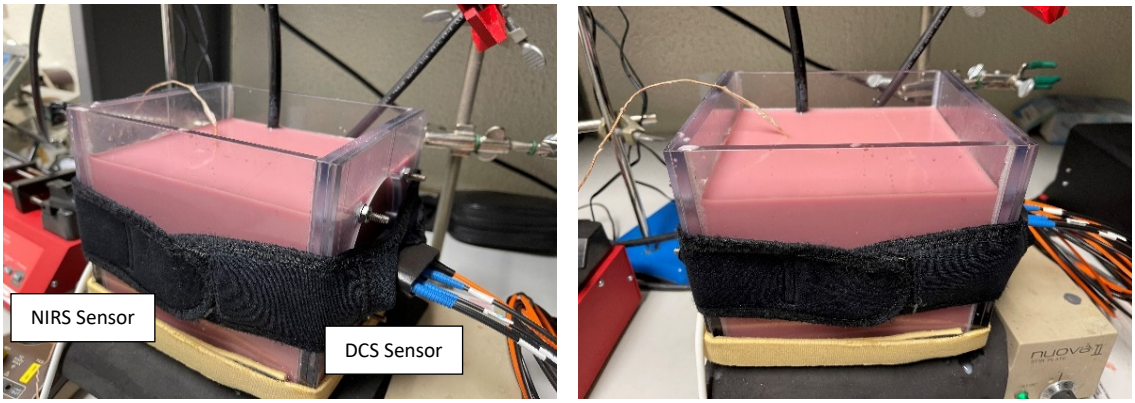

Figure 14. Blood phantom for oxygenation test with DCS and NIRS sensors/probes.

In this oxygenation test, the μ_s' is expected to stay constant since the concentration of the scatterers do not change. However, during the oxygenation (HbO2) and deoxygenation (Hb) stages, the amounts of absorbers in terms of the HbO2 and Hb vary and hence the absorption, μ_a in the medium is expected to change. These alterations in μ_a is expected to detected by the NIRS device in its extracted HbO2 and Hb measurements but should not affect DCS and its BFi measurements. *With this oxygenation test, we evaluated simultaneously recorded DCS and NIRS data and their extracted parameters under varying oxygen saturation conditions.*

NIR Device Measurements – Intensity, Hemoglobin and Water (Edema) Concentrations: We report the intensity measurements as recorded by the existing NIRS device at 730, 850 and 940nm wavelengths from its detectors at (a) 25 and (b) 33 mm SDS where the 1st and 2nd vertical lines indicate the start of the deoxygenation and reoxygenation stages, respectively (Figure 15)

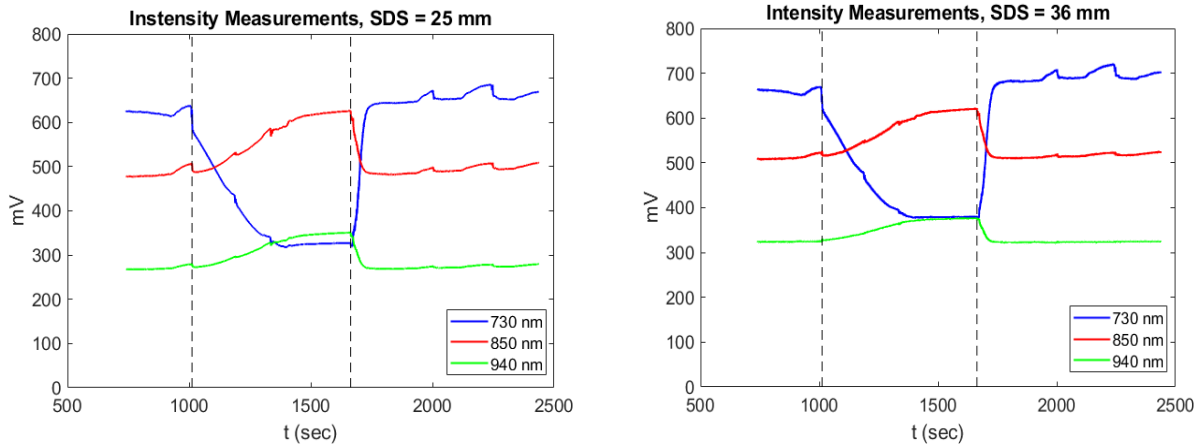

Figure 15. NIRS intensity measurements for light sources at 730, 850 and 940 nm wavelengths measured from detectors at different source detector separations (SDS) during oxygenation test.

It can be clearly observed from Figure 15 that the measured light intensity at all three wavelengths, which aims to detect the contributions from various tissue absorbers, changed during ***deoxygenation*** and ***reoxygenation*** stages. The main absorbers in the liquid phantom employed during this test were the hemoglobin in oxygenated and deoxygenated forms (HbO2, Hb) and water. *Notably, those are the absorbers whose concentrations can get altered as a result of different types of injuries such as hypoxia, ischemia or edema development.* Hence, we were interested in extracting the changes in the concentrations of HbO2, Hb and the total hemoglobin (HbT=HbO2+Hb) water content using NIRS technology (see also Figure 16).

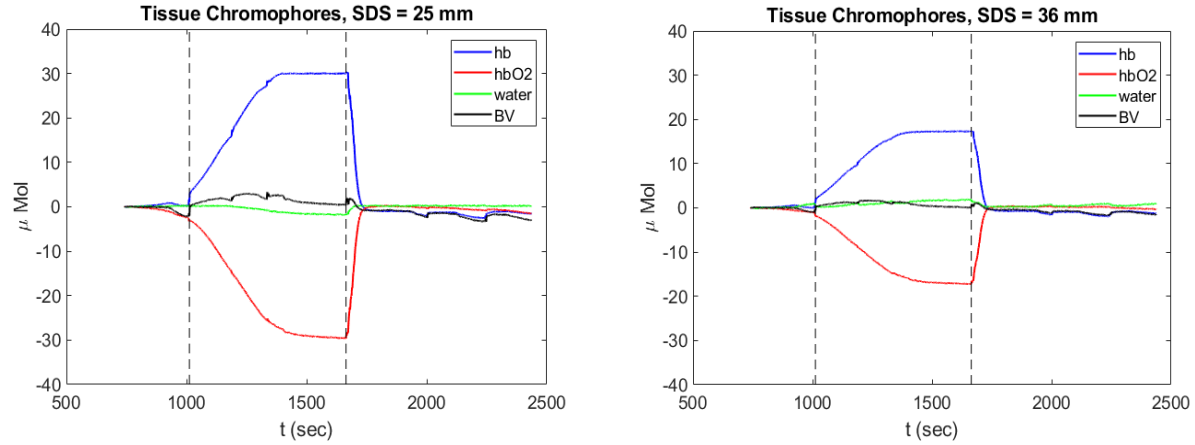

Figure 16. Extracted tissue chromophore concentrations (ΔC_{Hb}, ΔC_{HbO2}, ΔC_{HbT}, and ΔC_{water}) measured from detectors at 25 and 36 mm SDS during oxygenation test.

This test has shown that our algorithms and parameters are appropriate for the extraction of ΔC_{Hb}, ΔC_{HbO2}, ΔC_{HbT}, and ΔC_{water} from NIRS measurements and can provide information on regional tissue oxygen saturation changes, blood loss and edema development.

Blood Flow Measures using DCS System - BF_i*:* We present the estimated blood flow index, BF_i values from the device measurements at each SDS, during the whole oxygenation testing session in Figure 17, where vertical lines represent the start of ***deoxygenation*** and ***reoxygenation*** stages. Note

that the details how blood flow index was calculated, is provided in ***Appendix A***. These results reveal that when oxygen saturation changes from >90% to <10% levels and back which can cause changes in absorption (μ_a) throughout the test, there was not much change in blood flow index, BF_i. This is expected because change in BF_i due to absorption was small, main contributor to blood flow changes were due to scattering as we tested and shown in this report.

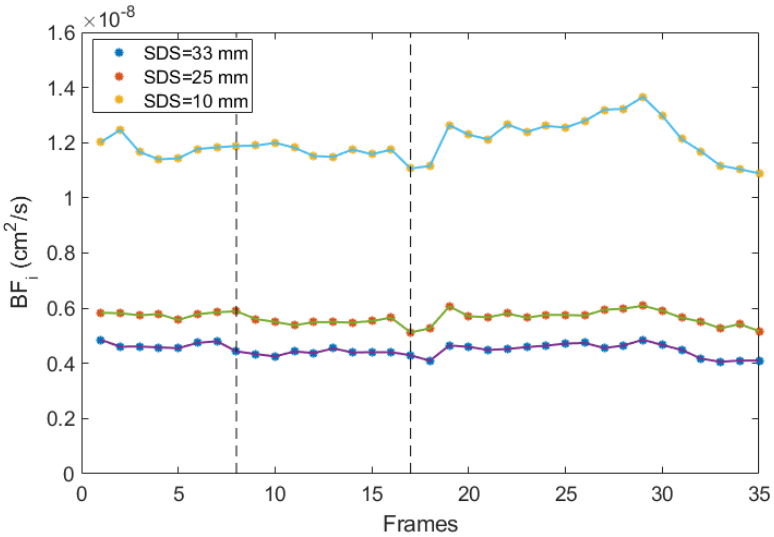

Figure 17. Estimated BF_i from DCS data from detectors throughout the overall oxygenation test where vertical lines represent the start deoxygenation and reoxygenation stages.

Discussion on Subtask 1.4.a and 1.4b: The phantom tests validated that the system and algorithm, developed under this award to monitor cerebral blood flow and cerebral oxygenation:

- ✓ passed the linearity tests, medium scattering and flow speed rate tests, and
- ✓ were able to assess the changes in response varying flow rates with constant depth of penetration to the tissue as well as varying flow rates under different depth of penetration (depth of penetration to the tissue is achieved by designing multiple optical source detector separations - SDSs)
- ✓ were able to detect changes in response to varying oxygenation changes. Combined NIRS and DCS system probes/sensors were used and detected changes in blood flow and in the concentrations of oxygenated hemoglobin (HbO2), deoxygenated hemoglobin (Hb), water and the total hemoglobin (HbT=HbO2+Hb). Notably, those are the main absorbers (biomarkers) whose concentrations can get altered as a result of different types of injuries, such as, hemorrhagic shock, hypoxia, ischemia or edema development.

Major Task 2. Test prototype in piglet model

Subtask 2.1: Prepare and submit the research protocol with animals for the review and approvals by IACUC and ACURO.

The study designs with piglets and adult pigs were developed and completed. Both research protocols were submitted. The IACUC and ACURO approvals were received for the piglet model study.

Discussion (Stated goals which have not met): The goal of this task was met. We are ready to kick off piglet study as soon as we acquire all the necessary catheters and probes. The final step on this task is to revise the second IACUC protocol (adult pig study) per ACURO review requests.

Subtasks 2.2-2.4:
Not yet initiated

Major Task 3. Test prototype in adult pig model of controlled and uncontrolled hemorrhagic shock
The research protocol and IACUC submission were completed, but ACURO approval is pending. The tests are not yet initiated.

Describe the Regulatory Protocol and Activity Status as applicable**.**
Animal Use Regulatory Protocols
PROTOCOL(S): 2

			Enter information regarding number of subjects					
ACURO Protocol Number	**Protocol PI Name**	**Organization (Site)**	**# Target**	**# Screened**	**# Recruited**	**# Enrolled**	**# Completed**	**Other**
RC190294.e001	Dr. Shadi Malaeb	Drexel University	30	0	0	0	0	
RC190294.e002	Dr. Dean Nachman	Hebrew University	20	0	0	0	0	
This annual reporting period			0	0	0	0	0	
Cumulative			50					

Protocol (1 of 2 total):

Protocol [ACURO Assigned Number]: RC190294.e001

Title: Portable Diffuse Optical Sensors for Point-of-Care Monitoring in Prolonged Field Care

Target required for statistical significance: 30

Target approved for statistical significance: 30

Submitted to and Approved by:

Provide bullet point list of protocol development, submission, amendments, and approvals (include IACUC in addition to ACURO).

Protocol Development: This protocol was developed to conduct proof of concept study and system tests in piglets. The experimental procedures and interventions, i.e., graded hemorrhage, fluid resuscitation, and induction of hypoxia ischemia are described in detail and reviewed.

Submission and Approvals: The protocol was first submitted to the Drexel University Institutional Animal Care & Use Committee and approved by the IACUC (*IACUC Protocol Number: 20889*) The protocol was reviewed and approved by the US Army Medical Research and Development Command (USAMRDC) Animal Care and Use Review Office (ACURO Protocol Number: RC190294.e001) on 10/15/2020.

Amendments: None

Status:

Progress Status: Not Yet Initiated.

Number of animals recruited/original planned target: 0 / 30

Number of animals enrolled/original planned target: 0 / 30

Number of animals completed/original planned target: 0 / 30

Protocol (2 of 2 total):

Protocol [ACURO Assigned Number]: RC190294.e002

Title: Portable Diffuse Optical Sensors for Point-of-Care Monitoring in Prolonged Field Care

Adult Pig Models for Real-life Clinical Scenario

Target required for statistical significance: 20

Target approved for statistical significance: 20

Submitted to and Approved by:

Provide bullet point list of protocol development, submission, amendments, and approvals (include IACUC in addition to ACURO).

Protocol Development: This protocol has been developed to conduct validation tests with adult pig models mimicking real-life clinical scenario. The experimental procedures including uncontrolled hemorrhage by liver laceration are described in detail and will be reviewed.

Submission and Approvals: The protocol was first submitted to the Hebrew University Institutional Animal Care & Use Committee and approved by the IACUC (*IACUC Protocol Number: MD-21-16440-3).* The protocol was submitted to the US Army Medical Research and Development Command (USAMRDC) Animal Care and Use Review for review and approvals.

Amendments: None

Status:

Progress Status: Not Yet Initiated.

Number of animals recruited/original planned target: 0 / 20

Number of animals enrolled/original planned target: 0 / 20

Number of animals completed/original planned target: 0 / 20

Administrative, Technical or Logistical issues: IACUC approval was received, and the protocol was submitted to US Army Medical Research and Development Command (USAMRDC) Animal Care and Use Review and the team received the feedback and has been working on the revised version.

What opportunities for training and professional development has the project provided?

If the project was not intended to provide training and professional development opportunities or there is nothing significant to report during this reporting period, state "Nothing to Report."

Nothing to Report

How were the results disseminated to communities of interest?
The team has not disseminated these new development and test results yet. We will prepare a manuscript for a journal to report these models, implementation of the algorithms and test results which are very promising.

What do you plan to do during the next reporting period to accomplish the goals?

We will accomplish following goals for the next annual reporting period:
Year 2 Quarter 1:

- Complete tests of software and hardware integration modules with all the boards designed in Year 1
- Complete simultaneous DCS and NIRS measures in phantom models for hypoxia, ischemia, and edema development.

Year 2 Quarter 2:
- Test using piglet model of graded hemorrhage
- Analyze physiological data and DCS and NIRS signal synchrony in response to change in the phase of hemorrhagic shock
- Modify the sensor prototype based on the piglet tests

Year 2 Quarter 3:
- Test using a piglet model of hypoxia-induced cerebral edema
- Analyze to determine the relationship between changes in DCS and NIRS signals of cerebral and somatic tissue oxygen saturation, cerebral edema, cerebral blood flow and changes in intracranial pressure (ICP) and pulse oximetry.
- Analyze physiological data and DCS-NIRS signal synchrony in response to edema development

Year 2 Quarter 4:
- Test the prototype in an adult pig model of controlled hemorrhagic shock and uncontrolled hemorrhage by liver laceration.
- Analyze and report validation analysis using physiological data and DCS and NIRS signal synchrony in response to change in the phase of hemorrhagic shock during this clinical model

4. IMPACT:

There are critical findings and major accomplishment even though we are at the early phase of this project. Using same modality, i.e., optics, with implementation of two different techniques, namely near infrared spectroscopy (NIRS) and diffuse correlation spectroscopy (DCS) techniques, multiple biomarkers were extracted and tested via novel and dynamic phantom models. All these models were custom designed, developed and enable us to control and mimic various physiological and physical changes in medium (tissue).

What was the impact on the development of the principal discipline(s) of the project?

The techniques of biomedical optics and sensors were extended in this project by combining power of the measures tuned to cerebral blood flow changes, cerebral blood volume changes, and concentration changes in local tissue oxygenation and water content (edema). A dedicated, fully operational DCS system was built under this award and implemented throughout the tests. A custom algorithm was developed to track changes in blood flow and blood volume.

In summary, the team was able to determine and test the changes in blood flow, deoxygenation, oxygenation, total hemoglobin (blood volume) and water (BF_i, ΔC_{Hb}, ΔC_{HbO2}, ΔC_{HbT}, and ΔC_{water} respectively). These biomarkers can provide information on blood loss, regional tissue oxygen saturation changes, water, and more importantly they are the main absorbers (biomarkers) whose concentrations can get altered as a result of different types of injuries, such as, hemorrhagic shock, hypoxia, ischemia or edema development.

What was the impact on other disciplines?

In general, ability to extract and assess various cerebral biomarkers can lend itself to design multiple combat casualty care capabilities and will help greatly improve diagnostic accuracy and guide better triage and treatments in austere environments. Specific to this period in this project, the test models we custom developed for this project can easily be used to test other clinical modalities or systems, such as efficacy and reliability of new local tissue oxygenation sensors which have been recently key sensory device in detecting some of COVID-19 symptoms. Decision making or regulatory agencies, such as the U.S. Food and Drug Administration can use these test models for independent evaluations. These models are modular, dynamic and can be easily tailored to mimic different tissue oxygenation, cerebral blood flow or water content changes for different injury types.

Use of the prototype system we are developing can also be extended to other clinical uses or field applications, such as depth of anesthesia and sedation monitoring for ambulatory anesthesia or cognitive state assessment - quantitative brain function evaluation in theater or in various field settings to monitor mission readiness or trainee's expertise development.

What was the impact on technology transfer?

Nothing to report for this period.

What was the impact on society beyond science and technology?

As previously mentioned, decision making or regulatory agencies, such as the U.S. Food and Drug Administration (FDA) can use these phantom test models for independent evaluations.

This project helps two new graduate students and one undergraduate engineering student to improve their knowledge and skills.

5. CHANGES/PROBLEMS:

Nothing to report.

Changes in approach and reasons for change

Nothing to report.

Actual or anticipated problems or delays and actions or plans to resolve them

We experienced following delays throughout Year 1:

- We experienced a problem in shipment: Due to COVID-19 and social distancing, we have been using domestic package carrier to transfer the hardware components and electronic modules from InfraScan, Inc. (subaward) to Drexel University. However, one key electronic module required for the DCS system was not delivered by the carrier. To resolve this issue: Subcontractor tracked this shipment, and able to receive the electronic module.
- We experienced delay in access to the machine shop capability: We customized enclosure and front panels for the proposed system, however we had to wait until machine shop personnel was back to their regular schedule.
- We continue to have delays in shipment (short of supply) and in some engineering services, such as board fabrication this quarter. For instance, the fluid channels (special tubes to model capillary) were acquired late, but still waiting mechanical designs and fabrication of the boards to complete the tests.
- The PI has also been working closely with clinical Co-Investigator to support logistics and scheduling required for the upcoming animal studies.

Changes that had a significant impact on expenditures

Nothing to report.

Significant changes in use or care of human subjects, vertebrate animals, biohazards, and/ or select agents

Significant changes in use or care of human subjects
Not applicable

Significant changes in use or care of vertebrate animals
Nothing to report.

Significant changes in use of biohazards and/or select agents
Nothing to report.

6. PRODUCTS:

- **Publications, conference papers, and presentations**

Journal publications. Nothing to report

Books or other non-periodical, one-time publications.
Nothing to report.

Other publications, conference papers and presentations.
Nothing to report.

- **Website(s) or other Internet site(s)**

  Nothing to report

- **Technologies or techniques**

  - A complete fully functional diffuse correlation spectroscopy (DCS) with a multi-distance optical probe/sensor and data acquisition software.
  - Algorithms implemented to determine blood flow and concentration changes in deoxygenation, oxygenation, total hemoglobin (blood volume) and water.

- **Inventions, patent applications, and/or licenses**

  Nothing to report

- **Other Products**

  Custom developed dynamic phantom models, techniques and set ups to mimic the changes in blood flow, deoxygenation, oxygenation, total hemoglobin (blood volume) and water

7. PARTICIPANTS & OTHER COLLABORATING ORGANIZATIONS

What individuals have worked on the project?

Name:	Kurtulus Izzetoglu
Organization:	Drexel University
Project Role:	PI
Researcher Identifier (ORCID ID):	0000-0001-5304-7361
Nearest person month worked:	5.0
Contribution to Project:	Dr. Izzetoglu has been leading overall conduct of the project and ensure the successful completion of the SOW tasks, the efforts include but not limited to, development of devices, phantom models, tests and data analysis, and led internal technical team meetings, and report preparation.

Name:	Leonid Zubkov
Organization:	Drexel University
Project Role:	Co-Investigator
Researcher Identifier (ORCID ID):	0000-0001-6523-5984
Nearest person month worked:	4.2
Contribution to Project:	Dr. Zubkov has designed and developed DCS control box and system, optical fibers, and multi-distance probes. He has provided technical support for system setup during tests.

Name:	Shadi Malaeb
Organization:	Drexel University
Project Role:	Co-Investigator
Researcher Identifier (ORCID ID):	0000-0001-6523-5984
Nearest person month worked:	0.6
Contribution to Project:	Dr. Malaeb has performed work in the area of clinical studies, particularly in animal protocol development and submission for the IACUC and ACURO review and approvals. The PI and Dr. Malaeb have also been working on the logistics and acquisition of the required supplies, catheters and probes for the animal studies.

Name:	Juan Du
Organization:	Drexel University
Project Role:	Lab technician & manager
Researcher Identifier (ORCID ID):	0000-0002-7978-0665
Nearest person month worked:	12.0

Contribution to Project:	Ms. Juan Du built the dynamic and custom phantoms for cerebral blood volume and flow measures by using intralipids and conducted phantom test procedures. She has also designed all the test procedures and conducted the tests.
Name:	Konur Bayrak
Organization:	Drexel University
Project Role:	Graduate student
Researcher Identifier (ORCID ID):	0000-0002-6589-9075
Nearest person month worked:	3.0
Contribution to Project:	Mr. Konur had assisted device development, signal processing algorithms for DCS system.
Name:	Prat Reddy
Organization:	Drexel University
Project Role:	Graduate student (PhD)
Researcher Identifier (ORCID ID):	0000-0002-6589-9075
Nearest person month worked:	6.0
Contribution to Project:	Ms. Prat has been assisting lab tests and has been working on signal processing algorithms for cerebral blood flow and volume measures.
Name:	Baruch Ben Dor
Organization:	InfraScan, Inc
Project Role:	Subaward PI
Researcher Identifier (ORCID ID):	*0000-0002-5531-8732*
Nearest person month worked:	2.8
Contribution to Project:	Dr. Ben Dor has been leading the subaward efforts for developing NIRS system.
Name:	David Solt
Organization:	InfraScan, Inc
Project Role:	Subaward co-Investigator (co-I)
Researcher Identifier (ORCID ID):	
Nearest person month worked:	3.3
Contribution to Project:	Mr. David has been supervising and developing NIRS system with flat probes and FPGA; working on the mechanical system design, integration and NIRS system with flat probes.
Name:	Gerald Mullin
Organization:	InfraScan, Inc
Project Role:	Subaward Electrical Engineer
Researcher Identifier (ORCID ID):	
Nearest person month worked:	3.3
Contribution to Project:	Mr. Gerry designed and developed a prototype lock-in amplifier with a FPGA module design. He has performed

work in software, specifically embedded coding of an FPGA module, as well.

Name: Anthony Groch
Organization: InfraScan, Inc
Project Role: Subaward Electrical Engineer
Researcher Identifier (ORCID ID):
Nearest person month worked: 2.8
Contribution to Project: Mr. Tony has performed work in development of an NIRS flat probes with LEDs and lock-in amplifier.

Name: Meltem Izzetoglu
Organization: Villanova University
Project Role: Subaward PI
Researcher Identifier (ORCID ID): 0000-0002-1768-3384
Nearest person month worked: 2.0
Contribution to Project: Dr. Meltem Izzetoglu assisted design of the test procedures and has analyzed phantom tests. She has also been working on algorithm development for the blood flow indices using measures of the optical sensors developed in this project.

Name	*Project Role*	*Organization*	*Calendar Months (Year 1)*	*Contribution to Project*
Kurtulus Izzetoglu	PI	Drexel University	*5.0*	Dr. Izzetoglu has been leading overall conduct of the project and ensure the successful completion of the SOW tasks, the efforts include but not limited to, development of devices, phantom models, tests and data analysis, and led internal technical team meetings, and report preparation.
Shadi Malaeb	Co-Investigator	Drexel University	0.6	Dr. Malaeb has performed work in the area of clinical studies, particularly in animal protocol development and submission for the IACUC and ACURO review and approvals. The PI and Dr. Malaeb have also been working on the logistics

				and acquisition of the required supplies, catheters and probes for the animal studies.
Leonid Zubkov	Co-Investigator	Drexel University	4.2	Dr. Zubkov has designed and developed DCS control box and system, optical fibers, and multi-distance probes. He has provided technical support for system setup during tests.
Juan Du	Technician	Drexel University	12.0	Built the dynamic and custom phantoms for cerebral blood volume and flow measures by using intralipids and conducted phantom test procedures. She has also designed all the test procedures and conducted the tests.
Konur Bayrak	Graduate Student	Drexel University	3.0	Assisting device development, signal processing algorithms for DCS system.
Prat Reddy	Graduate Student	Drexel University	6.0	Assisting lab tests and has been working on signal processing algorithms for cerebral blood flow and volume measures.
Baruch Ben-Dor	Subaward PI	InfraScan	2.8	Dr. Ben-Dor has been leading the subaward efforts for developing NIRS system
David Solt	Subaward Co-I	InfraScan	3.3	Supervising and developing NIRS system with flat probes and FPGA. Working on the mechanical system design, integration and NIRS system with flat probes
Gerald Mullin	Subaward Electrical Engineer	InfraScan	3.3	Designed and developed a prototype lock-in amplifier with a FPGA module design. He has performed work in software,

				specifically embedded coding of an FPGA module, as well.
Anthony Groch	Subaward Electrical Engineer	InfraScan	2.8	Performed work in development of an NIRS probes with LEDs and lock-in amplifier.
Meltem Izzetoglu	Subaward PI	Villanova University	2.0	Dr. Meltem Izzetoglu assisted design of the test procedures and has analyzed phantom tests. She has also been working on algorithm development for the blood flow indices using measures of the optical sensors developed in this project.

Has there been a change in the active other support of the PD/PI(s) or senior/key personnel since the last reporting period?

Nothing to report

What other organizations were involved as partners?

Organization Name: InfraScan, Inc
Location of Organization: (if foreign location list country) Philadelphia, PA
Partner's contribution to the project (identify one or more)

- Collaboration/Subcontractor: InfraScan, Inc. is a subawardee and the engineers have been developing the NIRS system including hardware and software development.

Organization Name: Hebrew University
Location of Organization: (if foreign location list country) Jerusalem, Israel
Partner's contribution to the project (identify one or more)

- Collaboration/Subcontractor: Hebrew University. is a subawardee and will develop adult pig animal models and experimental protocols and conduct these studies. Colleagues at the Hebrew University developed the research protocol during this Year 1.

Organization Name: Villanova University
Location of Organization: (if foreign location list country) Villanova, PA
Partner's contribution to the project (identify one or more)

- Collaboration/Subcontractor: Villanova University. is a subawardee and collaborating with lead institute on analyzing phantom tests reported during this year including linearity, scattering and flow speed tests. They have also been working on algorithm development for data analysis and blood flow indices using measures of the optical sensors developed in this project.

8. SPECIAL REPORTING REQUIREMENTS

COLLABORATIVE AWARDS:

QUAD CHARTS:

Updated quad chart is submitted.

9. APPENDICES:

Appendix A includes the algorithm developed for blood flow index calculation, additional test data, theoretical information, and the references cited.

APPENDIX A:

Blood Flow Index Algorithm Development, Data Analysis and Evaluation Using Phantom Tests

Theoretical Background: DCS measures the speckle fluctuations over time due to the moving scatterers in tissue (such as red blood cells -RBC), which is then used to estimate an index of blood flow in the microvasculature, namely the blood flow index (BF_i) (Tamborini et al., 2017). The motion information below the tissue surface is carried in the electric field of diffuse light and can be extracted from the electric field autocorrelation function which satisfies a correlation diffusion equation, $G_1(\rho,\tau)$ when $\mu_s' \gg \mu_a$ (Dong et al., 2012, Boas et al., 2016). The analytic solution of the correlation diffusion equation using Green's function for a point light source upon a semi-infinite medium is:

$$G_1(\rho,\tau) = \frac{3\mu_s'}{4\pi}\left\{\frac{e^{-K(\tau)r_1}}{r_1} - \frac{e^{-K(\tau)r_2}}{r_2}\right\} \quad (1)$$

Where τ is the delay time, ρ is the source detector separation, μ_s' is the reduced scattering coefficient, μ_a is the absorption coefficient, $r_1 = \sqrt{(\frac{1}{\mu_s'})^2 + \rho^2}$, $r_2 = \sqrt{\left(2z_b + \frac{1}{\mu_s'}\right)^2 + (\frac{1}{\mu_s'})^2 + \rho^2}$, $z_b = \frac{2}{3\mu_s'}\frac{1+R_{eff}}{1-R_{eff}}$, $R_{eff} = -1.44n^{-2} + 0.71n^{-1} + 0.668 + 0.064n$ is the effective reflection coefficient determined by the index of refraction which is the ratio of the refraction indices inside and outside of the medium and usually taken as $n \approx 1.33$ for biological tissues and $K(\tau) = \sqrt{3\mu_a\,\mu_s' + \mu_s'^2 k_o^2 \alpha \langle \nabla r^2(\tau)\rangle}$ where α is a unitless factor which represents the fraction of light scattering events from moving scatterers like RBCs, $k_o = 2\pi n/\lambda$ is the scattering wavevector which depends on the wavelength of light, λ and $\langle \nabla r^2(\tau)\rangle$ is the mean square displacement of the moving scatterers.

In biological tissues, $\langle \nabla r^2(\tau)\rangle$ is commonly described using two different models, namely the Brownian motion and random flow model. The Brownian motion model considers the motion of scatterers as diffusive motion and $\langle \nabla r^2(\tau)\rangle = 6D_B\tau$ where D_B is the effective diffusion coefficient of the scatterers. The random flow model assumes the random ballistic motion of scatterers and $\langle \nabla r^2(\tau)\rangle = \langle V^2\rangle\tau^2$ where $\langle V^2\rangle$ represents the mean square velocity of the scatterers (Dog et al, Yu et al.). Although the motion of RBCs may be considered as random flow physically, the Brownian motion model resulted in better representations of the measured autocorrelation functions for the majority of cases, ranging from brain to muscle and tumor models. Therefore, in DCS application, the measurements of $G_1(\rho,\tau)$ are fitted to the analytical solution mainly using the Brownian motion model to yield a blood flow index ($BF_i = \alpha D_B$) to parameterize the relative cerebral blood flow where $K(\tau) = \sqrt{3\mu_a\,\mu_s' + 6\mu_s'^2 k_o^2 \tau BF_i}$.

Experimentally, the measured intensity autocorrelation function, $g_2(\rho,\tau)$ is related to the normalized electric field autocorrelation function, $g_1(\rho,\tau) = G_1(\rho,\tau)/G_1(\rho,0)$ by the Siegert relation in the DCS systems, as follows:

$$g_2(\rho,\tau) = 1 + \beta|g_1(\rho,\tau)|^2 \quad (2)$$

where β is a constant determined primarily by the collection optics of the experiment. In most DCS systems, nonpolarized light sources and single mode fibers without polarizers are used in which case it is taken as $\beta \approx 0.5$, whereas if a polarizer is placed on a detector fiber, it can become $\beta \approx 1$ (Buckley et al, 2014, Durduran et al., 2014, Verdecchia et al., 2016, Tamborini et al., 2017).

Hence, in DCS applications, first the measured intensity autocorrelation function, $g_2^m(\rho,\tau)$ is obtained from each multi-distance detector at each time lag. Then, using the correlation diffusion equation formulation, $G_1(\rho,\tau)$ as given in equation (1), within equation (2), the calculated autocorrelation function formulation $g_2^c(\rho,\tau) = 1 + \beta|G_1(\rho,\tau)/G_1(\rho,0)|^2$ is obtained in terms of the variables, BF_i and β. Finally, the unknown BF_i and β values are estimated by fitting the analytically calculated autocorrelation function, $g_2^c(\rho,\tau)$ to the measured one, $g_2^m(\rho,\tau)$ ((Buckley et al, 2014, Durduran et al., 2014, Verdecchia et al., 2016) by minimizing the objective function:

$$\chi^2 = \sum[g_2^c(\rho,\tau) - g_2^m(\rho,\tau)]^2 \quad (3)$$

Blood Flow Index Extraction Under Various Flow Rates:

In Quarter 4, we developed the analysis codes that implement the aforementioned theory. In all our tests, the objective function given in equation (3) is minimized using the Nelder-Mead derivative free simplex method as provided in "fminsearch" function (Matlab 2019a Matworks, Natick, MA to estimate the BF_i and β from our DCS device $g_2^m(\rho,\tau)$ measurements using Brownian motion model. Once BF_i and β are estimated, we have also calculated the fitted $g_2^c(\rho,\tau)$.

In this test, we utilized the flow speed test data obtained in the Subtask 1.4.a and used the liquid phantom prepared with intralipid and water mixture providing μ_s'=6 cm^{-1} and μ_a =0.025 cm^{-1}. Note that for the circular tube of radius 0.08 cm as used in our microvasculature, the average channel flow speeds were calculated to be 0.07, 0.14 and 0.21 cm/s for the pump flow speeds of 50, 100 and 150 mL/h, respectively. The microvasculature was placed at 6 mm depth from the liquid phantom surface mimicking capillaries in the brain layer and the DCS probe was dipped in the liquid phantom, placed right at the surface level as shown in the Figure 8(b).

As shown in Figure 9, the decay time in $g_2(\tau)$ was increased with increasing flow rate. To quantify those changes in the autocorrelation curves and compare our DCS system measurements with studies in the literature as in (Tivnan et al., 2015), we extracted the suggested parameter in that work, $\tau_{½}$ for each flow-rate and presented $1/\tau_{½}$ in Figure A1(a). The parameter, $\tau_{½}$ was defined as the delay time when $g_2(\tau)$ was reduced to 50% of its full amplitude, where the full amplitude of $g_2(\tau)$ is given by the difference between its highest and lowest values. Since, the larger the $\tau_{½}$, the slower the flow; the reciprocal of $\tau_{½}$ was used as an indicator of the measured flow rates reflecting the experimental fact that autocorrelation traces decay faster for higher flow velocities. In Figure A1(b), we also compared our results with the ones from (Tivnan et al., 2015) where they were in agreement with each other. Note that SDS in Tivnan et al's study was 15 mm, shorter than the SDS of our device as shown here and hence the decay times were much faster in our measurements resulting in larger $1/\tau$ values.

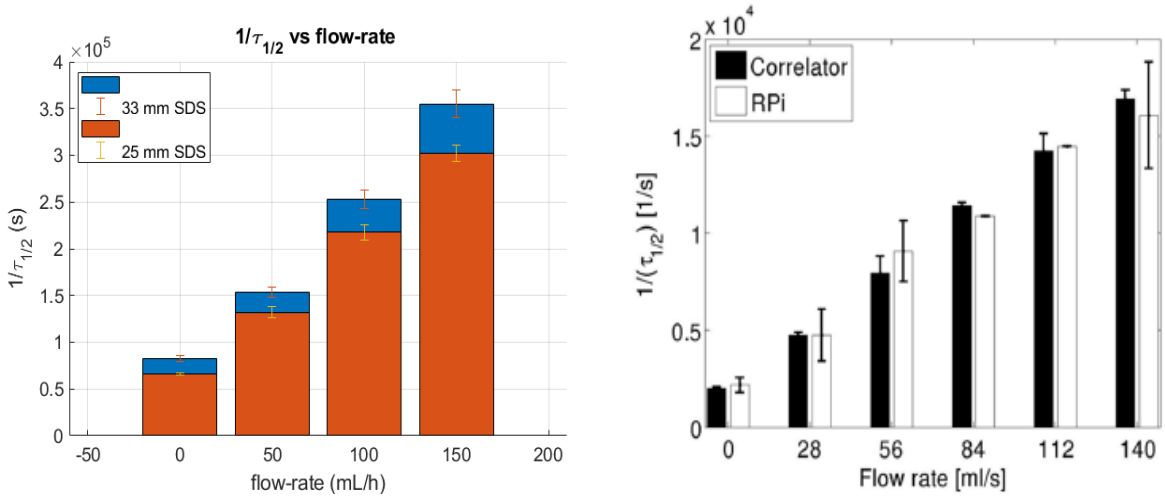

Figure A1. τ½ for each flow rate for (a) our DCS system and experimental setup; (b) results obtained from Tivnan et al. study.

Here, our goal was to test the validity and performance of our optimization and data fitting methods and codes developed to extract blood flow indices, which carry information about changes in cerebral blood flow (CBF). Note that, we performed the optimization procedure and minimized the objective function given in equation (3) only for the unknowns BF_i and β for each SDS, flow rate and frames, separately where μ_s' and μ_a are known values and taken exactly as the ones used in phantom preparation (μ_s'=6 cm^{-1} and μ_a =0.025 cm^{-1}). As example cases, the measured (dashed blue lines) and fitted (red solid lines) autocorrelation functions $g_2(\tau)$ at the detector with SDS of ρ =33 mm at different speeds at the first frame of recordings are shown in Figure A2.

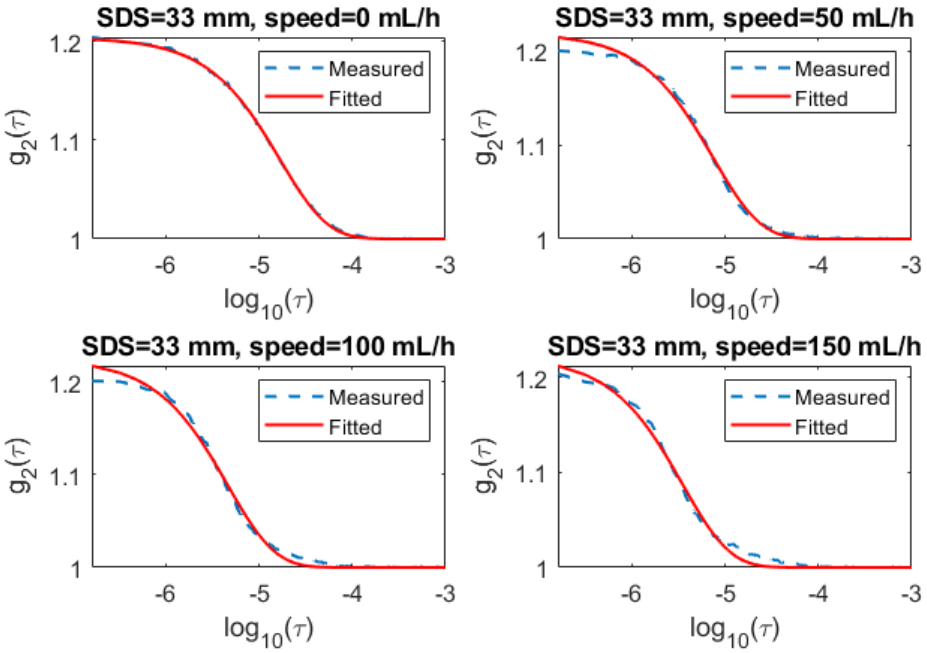

Figure A2. The logarithmic delay time ($\log_{10}(\tau)$) vs. the measured and fitted temporal autocorrelation function, $g_2(\tau)$ for different flow-rates at 0, 50, 100, and 150 mL/h, at the detector with 33 mm SDS.

The measured and fitted $g_2(\tau)$ followed similar patterns and look comparable visually having similar trends as in published results. To quantitatively compare these outcomes, we have obtained correlation coefficient, R and root mean square error (RMSE) for all cases of flow rate and SDS. Table 1 below summarized the mean ± standard deviation (std) values obtained using the available frames in each case. The very low RMSE values and strong positive correlation between the measured and fitted $g_2(\tau)$ values show that *i) for known scattering (μ_s') and absorption (μ_a), the estimated values determined using optimization techniques (analytical solution) significantly match the measured values acquired by our device, ii) Brownian motion model holds in our phantom tests; iii) our code was correctly implemented, and can be effectively used to extract the BF_i.*

Table 1: RMSE and correlation coefficient values between the measured and fitted $g_2(\tau)$

	SDS = 10 mm	SDS = 25 mm	SDS = 33 mm
Flow rate=0 mL/h	RMSE=0.0084±0.0017 R=0.999±0.00003	RMSE=0.0162±0.0024 R=0.999±0.00001	RMSE=0.01544±0.0011 R=0.999±0.00001
Flow rate=50 mL/h	RMSE=0.046±0.0014 R=0.996±0.0003	RMSE=0.081±0.0023 R=0.998±0.00006	RMSE=0.0447±0.0022 R=0.998±0.00008
Flow rate=100mL/h	RMSE=0.073±0.004 R=0.999±0.0006	RMSE=0.1157±0.0057 R=0.996±0.0002	RMSE=0.0537±0.0024 R=0.997±0.0001
Flow rate=150mL/h	RMSE=0.089±0.0029 R=0.982±0.001	RMSE=0.1517±0.0058 R=0.993±0.0005	RMSE=0.0647±0.0027 R=0.995±0.0004

Next, our aim was to test if our DCS system and its analysis algorithms were able to extract measures, primarily based on BF_i that can accurately and reliably differentiate change in flow rate. In Figure A3(a) and (b), we present the estimated BF_i values for each SDS, respectively where four intervals separated by vertical dashed lines represent the periods where the flow rate inside the microvasculature model is kept at 0, 50, 100 and 150 mL/h consecutively. The main observation from these results is that *when the flow rate increased (after each vertical dashed line), there was an increase in BF_i as would be expected*.

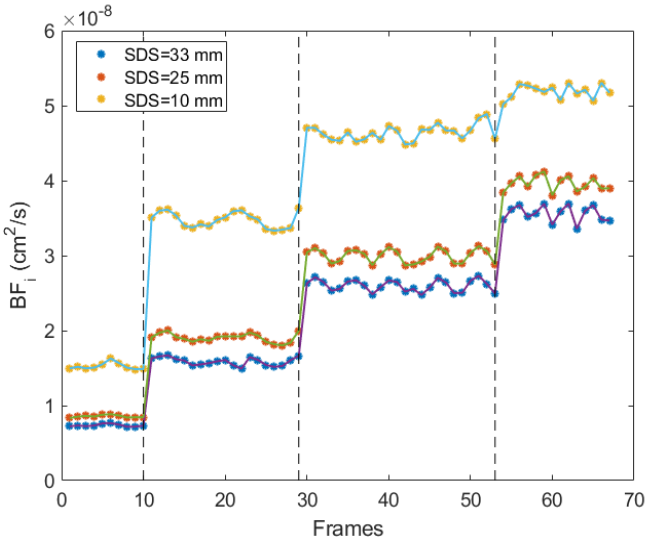

Figure A3. Estimated BF_i values in all frames of measured data throughout the overall experimental procedure where flow rate was changed from 0 to 50, 100 and 150 mL/h. These flow rate changes are represented by the vertical dashed lines at different depth of penetration achieved by varying the light source and detector separations (SDS).

Since use of DCS system enables us to measure changes in blood flow related to various disease or injury conditions and BF_i is the physiologically relevant biomarker that can provide blood flow changes, we focused on the algorithm to compute BF_i. In prior DCS studies relative changes in BF_i (rBF_i) at a certain time, which is defined as rBF_i = $BF_i/BF_{i,o}$, where $BF_{i,o}$ denotes the blood flow index at baseline, is also used for the comparison different conditions. To eliminate the static bias in BF_i estimations at different detectors as presented in Figure A4(a) and to compare the BF_i estimations at different detectors with each other and in terms of the change in flow rate, we also extracted the rBF_i by taking the baseline condition when there is no flow (flow rate=0 mL/h) as shown in Figure A4(b).

The similarity in the results for measurements at 25 and 33 mm SDS is an expected outcome since the relative change in blood flow index as measured by the DCS device in relation to the actual flow rate of the blood in blood vessels should be the same for each detector and should be independent of SDS. We have observed that even though this expected result is apparent in detectors at 25 and 33 mm SDS, it did not hold for the detector measurements at 10 mm SDS. We believe this discrepancy is due to the selected depth of the microvasculature model at 6 mm from the surface. It is assumed and shown via Monte Carlo simulations (Izzetoglu et al., 2021) that the depth of penetration of light in tissue for NIRS based devices are approximately half of the light source detector separation (~ SDS/2). Hence, for the detector at 10 mm SDS, the depth of penetration of NIR light is approximately at 5 mm which may or may not fully reach the microvasculature model, resulting in slightly deviant results in this detector rBF_i estimations in comparison to the detectors at 25 mm and 33 mm SDS.

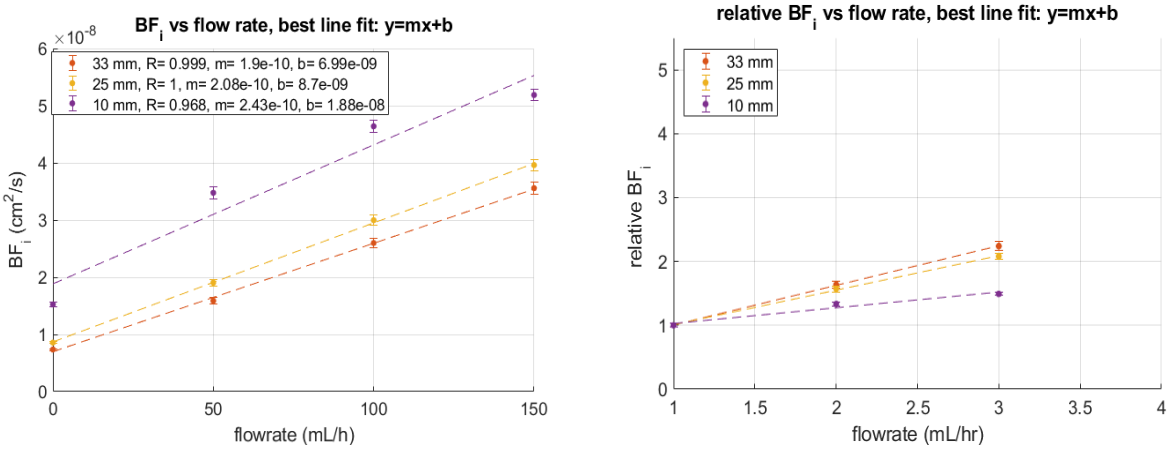

Figure A4. Estimated (a) BF_i and (b) rBF_i vs flow rate for detectors at 10, 25 and 33 mm SDS.

References Cited:

Boas, D. A., Sakadžić, S., Selb, J. J., Farzam, P., Franceschini, M. A., & Carp, S. A. (2016). Establishing the diffuse correlation spectroscopy signal relationship with blood flow. *Neurophotonics*, *3*(3), 031412.

Buckley, E. M., Parthasarathy, A. B., Grant, P. E., Yodh, A. G., & Franceschini, M. A. (2014). Diffuse correlation spectroscopy for measurement of cerebral blood flow: future prospects. *Neurophotonics*, *1*(1), 011009.

Durduran, T., & Yodh, A. G. (2014). Diffuse correlation spectroscopy for non-invasive, micro-vascular cerebral blood flow measurement. *Neuroimage*, *85*, 51-63.

Dong, J., Bi, R., Ho, J. H., Lee, K., Thong, P. S., & Soo, K. C. (2012). Diffuse correlation spectroscopy with a fast Fourier transform-based software autocorrelator. Journal of biomedical optics, 17(9), 097004.

Izzetoglu, M., Pourrezaei, K., Du, J., & Shewokis, P. A. (2021). Evaluation of Cerebral Tissue Oximeters Using Multilayered Dynamic Head Models. IEEE Transactions on Instrumentation and Measurement, 70, 1-12.

Tamborini, D., Farzam, P., Zimmermann, B. B., Wu, K. C., Boas, D. A., & Franceschini, M. A. (2017). Development and characterization of a multidistance and multiwavelength diffuse correlation spectroscopy system. *Neurophotonics*, *5*(1), 011015.

Tivnan, M., Gurjar, R., Wolf, D. E., & Vishwanath, K. (2015). High frequency sampling of TTL pulses on a Raspberry Pi for diffuse correlation spectroscopy applications. Sensors, 15(8), 19709-19722.

Verdecchia, K., Diop, M., Lee, A., Morrison, L. B., Lee, T. Y., & Lawrence, K. S. (2016). Assessment of a multi-layered diffuse correlation spectroscopy method for monitoring cerebral blood flow in adults. *Biomedical optics express*, *7*(9), 3659-3674.

Vishwanath, K., & Zanfardino, S. (2019). Diffuse Correlation Spectroscopy at Short Source-Detector Separations: Simulations, Experiments and Theoretical Modeling. Applied Sciences, 9(15), 3047.

Wang, D., Gao, P., Zhu, L., Peng, Q., Li, Z., & Zhao, J. (2019). Optimization of detected optical intensity for measurement of diffuse correlation spectroscopy: Intralipid phantom study. AIP Advances, 9(1), 015315.